

SynLiDAR: Learning From Synthetic LiDAR Sequential Point Cloud for Semantic Segmentation

Aoran Xiao, Jiaxing Huang, Dayan Guan, Fangneng Zhan, Shijian Lu
School of Computer Science Engineering, Nanyang Technological University

{Aoran.Xiao, Jiaxing.Huang, Dayan.Guan, fnzhan, Shijian.Lu}@ntu.edu.sg

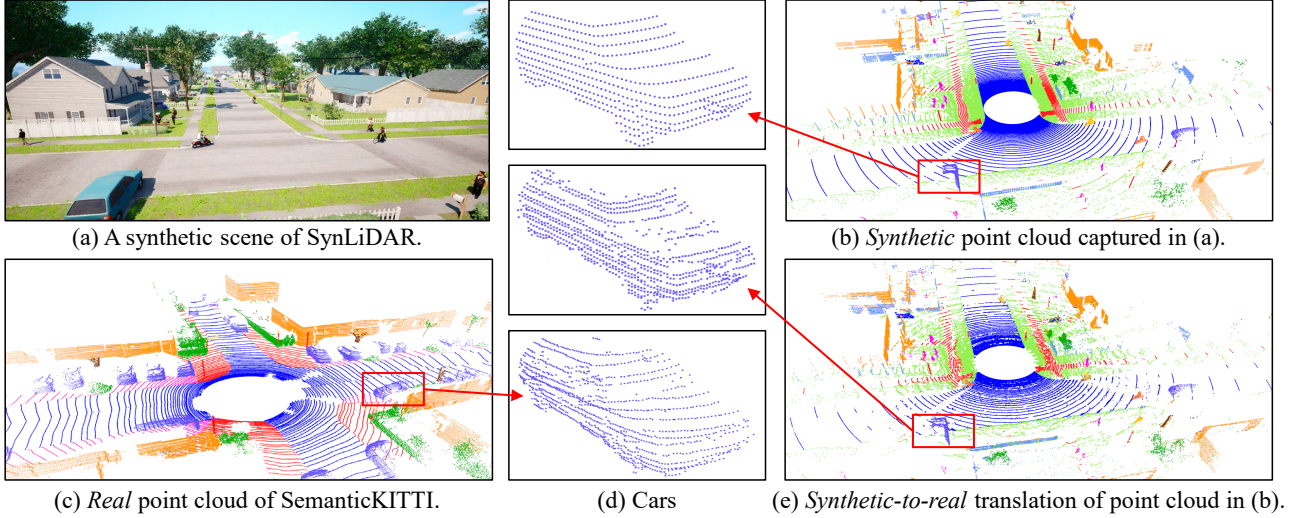


Figure 1: We create a large-scale multiple-class synthetic LiDAR point cloud dataset SynLiDAR with point-wise annotations as illustrated in (b) by constructing multiple virtual environments and 3D object models as illustrated in (a). To mitigate the domain gap with real-world LiDAR point cloud in (c), we design a point cloud translation network (PCT-Net) that transfers the geometry and sparsity styles of real data to SynLiDAR to produce a translated SynLiDAR in (e) that has similar distributions as real data and is more effective in model training. The close-up views in (d) show the translation effects. The dataset is available at <https://github.com/xiaoaoran/SynLiDAR>.

Abstract

Transfer learning from synthetic to real data has been proved an effective way of mitigating data annotation constraints in various computer vision tasks. However, the developments focused on 2D images but lag far behind for 3D point clouds due to the lack of large-scale high-quality synthetic point cloud data and effective transfer methods. We address this issue by collecting SynLiDAR, a synthetic LiDAR point cloud dataset that contains large-scale point-wise annotated point cloud with accurate geometric shapes and comprehensive semantic classes, and designing PCT-Net, a point cloud translation network that aims to narrow down the gap with real-world point cloud data. For SynLiDAR, we leverage graphic tools and professionals who construct multiple realistic virtual environments with rich scene types and layouts where annotated LiDAR points can be generated automatically. On top of that, PCT-Net dis-

entangles synthetic-to-real gaps into an appearance component and a sparsity component and translates SynLiDAR by aligning the two components with real-world data separately. Extensive experiments over multiple data augmentation and semi-supervised semantic segmentation tasks show very positive outcome - including SynLiDAR can either train better models or reduce real-world annotated data without sacrificing performance, and PCT-Net translated data further improve model performance consistently.

1. Introduction

Semantic segmentation of LiDAR sequential point cloud is critical in various scene perception tasks and it has attracted increasing attention from both industry and academia [5, 32, 33, 19, 44] in recent years. However, training effective segmentation models requires large amounts of annotated point cloud, which are prohibitively time-

dataset	format	#scans	#points	#classes	annotation	type
SemanticKITTI [5]	point	43,552	4,549M	25	point-wise	real
SemanticPOSS [33]	point	2,988	216M	14	point-wise	real
nuScenes-Lidarseg [6]	point	40,000	1,400M	32	point-wise	real
GTA-LiDAR [47]	image	121,087	-	2	pixel-wise	synthetic
PreSIL [22]	point	51,074	3,135M	2	point-wise	synthetic
SynLiDAR (ours)	point	198,396	19,482M	32	point-wise	synthetic

Table 1: Overview of outdoor LiDAR sequential point cloud datasets with semantic annotations: #scans: Number of scans for the datasets; #points: Number of points in millions (M); #classes: Number of semantic classes.

consuming to collect due to the view change of 3D data and visual inconsistency between LiDAR point cloud and physical world. This can be observed by the small size of existing *Real* LiDAR sequential datasets as listed in Table 1.

Inspired by the great success of transfer learning from synthetic to real data in two-dimensional (2D) field [38, 4, 13], one possible way to mitigate the data annotation constraint is to leverage synthetic point cloud data that can be collected and annotated automatically by computer engines. However, collecting large-scale synthetic LiDAR sequential point cloud is a nontrivial task which involves a large number of virtual scenes and objects as well as complicated point generation processes. In addition, most existing transfer learning methods [43, 41, 25, 40, 48] focus on 2D images which do not work for 3D point cloud. To the best of our knowledge, few researches tackle the challenge of synthetic-to-real transfer of point cloud of nature scenes, largely due to the lack of large-scale synthetic data with accurate geometries and rich semantic annotations.

We address the aforementioned issues by collecting SynLiDAR, a large-scale LiDAR sequential point cloud dataset for facilitating the research of synthetic-to-real transfer learning, and designing PCT-Net, a pioneer point-cloud translation network for mitigating domain gaps between synthetic and real point cloud (as Fig. 1 shows). We collect SynLiDAR from multiple virtual environments constructed by professional 3D generalists leveraging advanced graphic tools, each of which contains configurable object models that are similar to real-world data in geometry and layout. It is ideal for synthetic-to-real studies as it consists of comprehensive and diverse data (32 semantic classes with over 19 billion point-wise annotated points as illustrated in Fig. 2) and its collected points are highly accurate in geometry.

On top of SynLiDAR, PCT-Net disentangles the synthetic-to-real domain gap into an appearance component and a sparsity component. It consists of an appearance translation module that first translates synthetic point cloud into the intermediate representation with real appearance, as well as a sparsity translation module that learns the sparsity of real-world point cloud and further translates the intermediate representation into the final output that have similar

appearance and sparsity as real point cloud data.

The contribution of this work can be summarized in three aspects. First, we created SynLiDAR, a large-scale synthetic LiDAR sequential point cloud dataset that has rich semantic classes and a large number of points with accurate point-wise annotations. Second, we proposed PCT-Net, a point cloud translation network that can translate synthetic point clouds to have similar features and distributions as real-world point clouds and accordingly mitigate the domain gap between synthetic and real point clouds effectively. To the best of our knowledge, PCT-Net is the first translation network for LiDAR sequential point cloud. Third, we performed extensive studies and show that SynLiDAR shares high-similarities with real-world data and can supplement real-world data effectively in different manners. PCT-Net mitigates domain gaps between SynLiDAR and real point cloud and its translated data train better point-cloud segmentation models consistently.

2. Related Works

2.1. Semantic Point Cloud Segmentation

3D deep learning [17] has attracted increasing attention, which is important for different LiDAR perception tasks including semantic segmentation. Different approaches have been proposed to segment LiDAR point clouds. For example, projection-based methods project LiDAR point cloud into depth images and feed them to 2D CNNs for segmentation [47, 48, 32, 52, 24]. Point-based methods process point clouds directly by using the symmetric function [35, 36, 19]. Based on the sparsity of point clouds, several works propose sparse convolutions to accelerate computation [16, 9]. [16, 18, 51] use voxelization and apply regular 3D convolutions for segmentation. Some studies [29, 44] analyse the bottleneck of point-based and voxel-based methods and propose point-voxel convolution that combines both of them. [45, 56] proposed customized 3D convolution networks and achieved impressive performance.

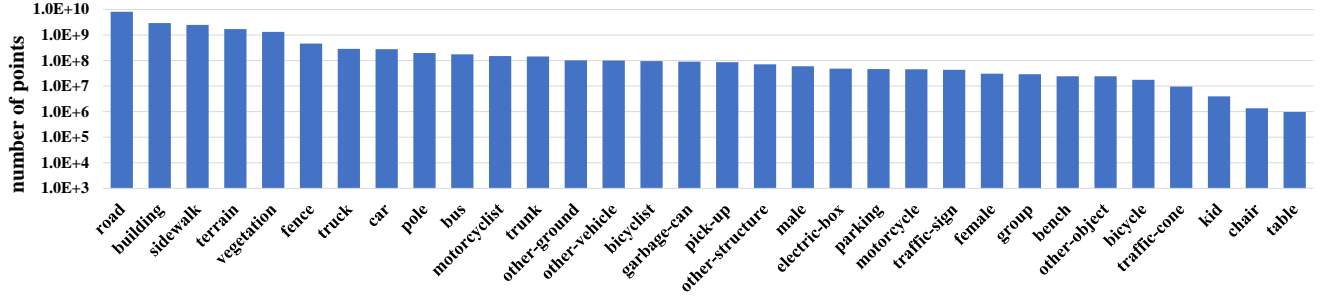


Figure 2: Point distribution in our proposed SynLiDAR: The 32 bars show the number of LiDAR cloud points of 32 semantic classes that are collected in SynLiDAR.

2.2. LiDAR Sequential Point Cloud Datasets

LiDAR *sequential* point clouds provide point cloud scans, each containing sparse and incomplete points collected in a sweep by LiDAR sensors. SemanticKITTI [5] is the first real dataset with point-wise annotations, which greatly promotes the development of LiDAR point cloud segmentation. The recently released SemanticPOSS [33] and nuScenes-Lidarse [6] enrich the diversity of LiDAR data resources. However, labeling point-wise semantic annotations is prohibitively time-consuming for LiDAR sequential point clouds. Therefore, existing real point cloud datasets have very limited data sizes as listed in Table 1.

Inspired by the success of 2D synthetic image datasets [37], a few pioneer studies [47, 22] have explored to collect synthetic point cloud data from GTA-V games. However, 3D meshes in GTA-V games are not accurate, e.g. pedestrians always downgrade into cylinders [47]. In addition, GTA-V games provide only two object classes *Car* and *Pedestrian*. Its collected synthetic data are thus insufficient for studying fine-grained LiDAR point cloud segmentation. We instead construct a wide range of realistic virtual environments and object models by leveraging graphic tools and professionals. The synthetic point clouds within the SynLiDAR thus capture much more accurate geometries and the rich diversity of semantic labels as in natural scenes.

2.3. Domain Translation

Domain Translation aims to learn meaningful mapping across domains. It is well developed for 2D images between paired domains [23, 46], unpaired domains [54, 31, 8, 28], multiple modalities [55, 20], etc. For 3D data, some attempt has been reported for translation from images to depth [27, 53], from point cloud to depth [39], from point cloud to images [11, 34], etc. However, the translation between point clouds of different domains is largely neglected. We address this challenge for mitigating the gap between synthetic and real point clouds.

3. The SynLiDAR Dataset

This section presents the proposed SynLiDAR dataset. It consists of three parts about virtual scene construction and data collection, intensity rendering, and dataset statistics and analysis, more details to be described in the ensuing three subsections.

3.1. Virtual Scenes & Data Collection

SynLiDAR is collected by rendering virtual scenes that are constructed by professional 3D generalists by using Unreal Engine 4 platform [2]. The virtual scenes include different types of outdoor environments such as cities, towns, harbour, etc. The dataset also contains a large number of physically accurate object models that are produced by expert modelers with 3D-Max software. We employ existing LiDAR sensor simulators [42, 50, 30] and set them as the same parameters as the Velodyne HDL-64E as used in SemanticKITTI [5] (64 beams channels in vertical field of view (FOV) between $[-25^\circ, 3^\circ]$, 100-meter working range, etc.). The point-cloud data is collected in complete 360° horizontal FOV in 10Hz frequency.

Note that SynLiDAR can be easily expanded by including new virtual scenes, 3D objects of new classes, etc. With that, the corresponding point cloud with point-wise annotations can be generated with little effort. From the other end, we collect SynLiDAR for the task of semantic segmentation of LiDAR point cloud and study of transfer learning with point cloud data. The dataset can be easily extended for other tasks such as object detection [15], panoptic segmentation [5], etc.

3.2. Intensity Rendering

Intensity refers to laser signal strength received by LiDAR sensors, which is an important attribute of LiDAR point clouds. It is challenging to simulate point intensity while collecting synthetic data due to the complicated signal transmission, propagation and reception processes. In SynLiDAR, we address this issue by training a rendering

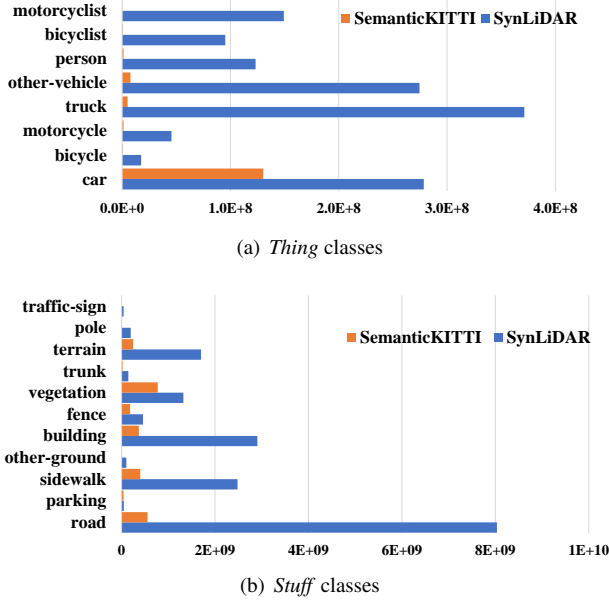


Figure 3: Numbers of annotated cloud points (X-axis) per class (Y-axis) for datasets SemanticKITTI and SynLiDAR.

model that learns from real LiDAR point cloud and predicts intensity values for SynLiDAR. Specifically, we train an intensity prediction model by using MinkowskiNet [10], where coordinates and semantic labels of cloud points in SemanticKITTI [5] are used as inputs and the point intensity (SemanticKITTI provided) is used as references.

3.3. Dataset Statistics and Analysis

SynLiDAR has 13 LiDAR point cloud sequences with point-wise annotations. Specifically, sequences 00-03, 04-06, 07-11, and 12 are collected from urban cities, suburban towns, neighborhood environments, and harbor, respectively. It has 198,396 scans of point cloud with 19 billion points in total, where each scan has around 98,000 points on average. Precise point-wise annotations of 32 semantic classes are provided for fine-grained scene understanding. Fig. 2 show point distributions of different classes.

SynLiDAR shares similar data imbalance issues as real datasets [5, 33] as illustrated in Fig. 2 since its constructed virtual scenes are similar to real-world environments. Some classes such as *road*, *sidewalk*, and *vegetation* have high occurrence frequencies while some classes such as *human* have lower frequencies (still with around 970,000 points per class). In addition, SynLiDAR is a truly *large-scale* point cloud dataset which has much more per-class points than SemanticKITTI (the largest real point cloud dataset to the best of our knowledge) as illustrated in Fig. 3.

4. Point Cloud Translation

Similar to most synthetic data, the LiDAR point cloud in SynLiDAR has a clear domain gap with real LiDAR data, and the model trained using SynLiDAR usually experiences clear performance drops while applied to real point clouds. An intuitive idea to mitigate the domain gap is to employ existing point cloud reconstruction models [49, 26, 7, 3, 21] to translate synthetic data to have real data distributions. However, existing supervisions such as Chamfer loss and Earth Mover’s Distance (EMD) cannot regularize sparsity distribution of LiDAR data and few researches tackle the challenge of point cloud translation either.

To address this issue, we design PCT-Net, a point cloud translation network that translates synthetic point clouds to have similar features as real point clouds. We disentangle synthetic-to-real gaps into an appearance component and a sparsity component [56] that encode the distribution of scene geometry and point sparsity, respectively. PCT-Net has an appearance translation module and a sparsity translation module that handle the two components as shown in Fig. 4. Note translating 3D LiDAR point cloud has been largely neglected (due to the lack of large-scale synthetic LiDAR data) though translating 2D images has been studied extensively in the computer vision research community. PCT-Net is probably the first such effort for the challenging scene semantic segmentation task to the best of our knowledge.

Given synthetic point clouds $X_s \in \mathbb{R}^{N_s \times 3}$ and real point clouds $X_r \in \mathbb{R}^{N_r \times 3}$, we aim to translate X_s into $\hat{X}_{s \rightarrow r} \in \mathbb{R}^{\hat{N}_s \times 3}$ that have similar appearance and sparsity as X_r . Given X_s , the appearance translation module first translates it to have certain *real* appearance by a generator G_A by $X'_s = G_A(X_s)$. The translated point cloud is then translated by the sparsity translation module to have certain *real* sparsity features by another generator G_S by $\hat{X}_{s \rightarrow r} = G_S(X'_s)$. More details of the two translation modules are provided in the ensuing two subsections.

Appearance translation module is a 3D generative adversarial network that consists of a generator G_A and a discriminator D_A which are trained in an adversarial manner. The generator aims to generate intermediate representation X'_s (from the original synthetic data) to have real appearance to fool the discriminator, while the discriminator learns to distinguish X'_s from X_r . Specifically, we up-sample X_t to an intermediate representation $U(X_t)$ so as to eliminate the effect of domain-specific sparsity features. The adversarial learning loss can be formulated as follows:

$$L_{adv \sim A} = \log(D_A(-G_A(X_s) \log(G_A(X_s)))) + \log(1 - D_A(U(X_t) \log(U(X_t)))) \quad (1)$$

We introduce EMD [12] for generator to keep same geom-

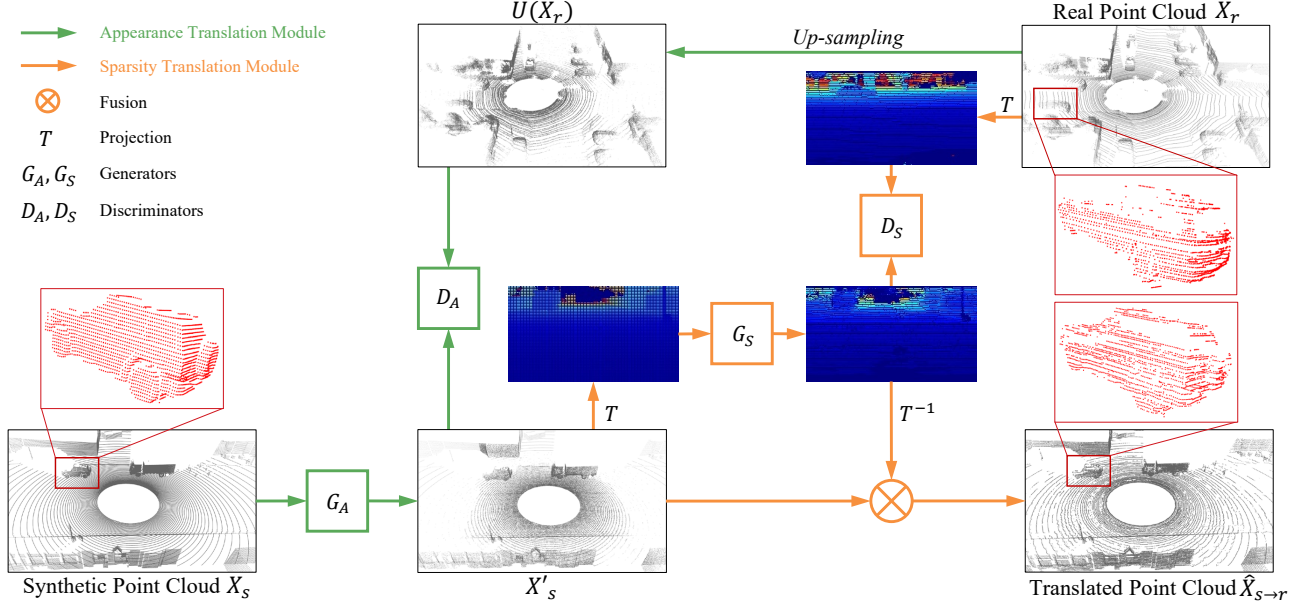


Figure 4: The proposed PCT-Net disentangles point-cloud translation into appearance translation and sparsity translation tasks. Given synthetic point cloud, the appearance translation module in PCT-Net first learns to reconstruct point cloud with real appearance. The sparsity translation module then learns real sparsity distribution in 2D space and fuses it with reconstructed point cloud in 3D space, leading to translated point cloud with real appearance and sparsity.

entry of X_s and X'_s

$$L_{EMD}(X_s, X'_s) = \sum_{x \in X_s} \|x - \phi(x)\|_2 \quad (2)$$

where $\phi : X_s \rightarrow X'_s$ is a bijection. The objective function of the appearance translation module can be formulated as:

$$L_A(G_A, D_A) = \arg \min_{G_A} \max_{D_A} (\lambda_{adv \sim A} L_{adv \sim A} + \lambda_{EMD} L_{EMD}) \quad (3)$$

Sparsity translation module aims to transfer sparsity information from real point cloud to synthetic point cloud. However, existing supervisions [12] such as Chamfer loss and EMD loss cannot capture sparsity information well as they lack sparsity regulation. To address this problem, we propose to first learn sparsity information in 2D space and then fuse it back into X'_s in 3D space. Specifically, we first project X'_s and X_t into depth images (as $T(X'_s)$ and $T(X_t)$ respectively), and then employ an image-to-image translation model to translate $T(X'_s)$ to have similar sparsity as $T(X_t)$. The translation network is also GAN-based with a generator G_S and a discriminator D_S . The adversarial learning loss can be formulated as follows

$$L_{adv \sim S} = \log(D_S(-G_S(T(X'_s))) \log(G_S(T(X'_s)))) + \log(1 - D_S(T(X_t) \log(T(X_t)))) \quad (4)$$

To preserve the geometry information during the translation, we further include a geometry consistency loss to ensure that the translated depth image preserves similar geometry as the original image:

$$L_{geo} = \|\overline{T(X'_s)} - \overline{G_S(T(X'_s))}\|_2 + \|\overline{T(X_t)} - \overline{G_S(T(X_t))}\|_2 \quad (5)$$

where $\overline{A} - \overline{B}$ means that the distance is computed for pixels existing in both A and B only. The overall objective of the sparsity translation module can be formulated by:

$$L_S(G_S, D_S) = \arg \min_{G_S} \max_{D_S} (\lambda_{adv \sim S} L_{adv \sim S} + \lambda_{geo} L_{geo}) \quad (6)$$

Finally, the translated image $G_S(T(X'_s))$ with real sparsity information are projected back into 3D space for fusion. Specifically, blank pixels in $G_S(T(X'_s))$ are used for guidance to drop out points in X'_s . The final output could be summarized as $\hat{X}_{s \rightarrow r} = [X'_s, T^{-1}(G_S(T(X'_s)))]$, where $[\cdot]$ represents the drop out process. The semantic labels of the translated point cloud are assigned according to labels of neighboring points in the original point cloud.

5. Experiments

We evaluate how SynLiDAR benefits semantic segmentation over multiple real point cloud datasets and state-of-the-art segmentation models. The experiments examine the

model	train	test	translation	car	bicycle	motorcycle	truck	other-vehicle	person	bicyclist	motorcyclist	road	parking	sidewalk	other-ground	building	fence	vegetation	trunk	terrain	pole	traffic-sign	mIoU
RandLA-Net	K	K	-	93.1	16.7	20.6	67.7	41.5	48.8	65.7	0.0	91.4	42.2	76.5	6.2	85.6	38.9	84.2	58.5	73.6	51.6	36.1	52.6
	K+S	K	-	94.1	19.7	28.7	73.6	46.4	46.1	66.6	0.0	91.7	39.9	76.8	3.1	86.9	39.1	84.1	60.1	72.7	50.2	39.5	53.6
	K+S	K	NDF [47]	94.4	19.6	28.1	72.9	46.5	48.4	68.6	0.0	91.5	40.2	77.2	2.7	87.3	41.6	85.2	58.8	72.1	51.0	37.8	53.9
	K+S	K	PCT-Net (our's)	94.7	20.1	30.4	72.1	50.4	49.1	65.7	0.0	91.9	43.3	77.5	3.3	87.8	45.5	86.5	61.3	75.4	53.6	38.4	55.1

Table 2: Incorporating SynLiDAR with real point cloud data trains better segmentation models: For RandLA-Net [19], including SynLiDAR into the SemanticKITTI [5] training data helps to train more accurate semantic segmentation models. ‘K’ and ‘S’ represent SemanticKITTI and SynLiDAR datasets. ‘NDF’ refers to noise distribution fixing method.

model	train	test	translation	car	bicycle	motorcycle	truck	other-vehicle	person	bicyclist	motorcyclist	road	parking	sidewalk	other-ground	building	fence	vegetation	trunk	terrain	pole	traffic-sign	mIoU
MinkNet	K	K	-	95.7	25.0	57.0	62.1	46.4	63.4	77.3	0.0	93.0	47.9	80.5	2.2	89.7	58.6	89.5	66.5	78.0	64.6	50.1	60.3
	K+S	K	-	96.1	28.2	59.1	68.0	50.0	68.4	80.5	0.0	93.3	47.4	80.8	2.7	90.2	60.4	89.5	67.5	77.7	64.9	50.4	61.8
	K+S	K	NDF [47]	96.1	28.7	59.6	73.1	49.4	66	80.1	0.0	93.9	50.8	81.3	3.5	89.4	59.9	90.3	66.1	82.2	62.4	50.5	62.3
	K+S	K	PCT-Net (our's)	95.6	33.1	62.6	74.3	49.1	70.2	83.0	0.0	94.3	55.7	81.8	1.9	90.2	59.8	88.0	67.3	81.8	65.2	50.7	63.4

Table 3: Incorporating SynLiDAR with real point cloud data trains better segmentation models: For MinkNet [10], including SynLiDAR into the SemanticKITTI [5] training data helps to train more accurate semantic segmentation models. ‘K’ and ‘S’ represent SemanticKITTI and SynLiDAR datasets. ‘NDF’ refers to noise distribution fixing method.

effectiveness of SynLiDAR in supplementing or replacing real data and how the proposed PCT-Net mitigates domain gaps between SynLiDAR and real point cloud data.

5.1. Datasets

We conduct experiments over two real-world point cloud datasets. The first is *SemanticKITTI* [5] that consists of 43,552 scans of annotated sequential LiDAR point cloud with 19 semantic classes. It is the largest real-world sequential LiDAR point cloud dataset for semantic segmentation to the best of our knowledge. We used sequences 00-07 and 09-10 for training and sequence 08 for testing. The second is *SemanticPOSS* [33] which is a newly released dataset collected on a university campus. It consists of 2,988 annotated point cloud scans of 14 semantic classes. We used sequence 03 for testing and the rest for training. Mean Intersection of Union (mIoU) is used as the evaluation metric.

5.2. Point Cloud Segmentation Models

We used two state-of-the-art segmentation networks each of which represents a typical point cloud processing approach. The first is *RandLA-Net* [19], a standard point-based method that uses raw point cloud scan as input and shares multiple layer perceptron (MLP) for feature extraction. To process large-scale point clouds efficiently, it uses random sampling to reduce computation time and memory

space. The second is *MinkowskiNet* [10], a sparse convolution network that adopts sparse tensors and sparse convolutions to process high-dimensional data effectively.

5.3. Implementation Details

For point cloud translation, we used PU-GAN [26] as the backbone in the appearance translation module and CycleGAN [54] in the sparsity translation module. Parameters $\lambda_{adv \sim A}$, λ_{EMD} , $\lambda_{adv \sim S}$, λ_{geo} are set at 0.01, 1, 5, 1, respectively. To train segmentation models, we first jointly train with real and synthetic data until convergence and then fine-tune using real data. For RandLA-Net, we use point coordinate as input features, and set learning rate at 0.01 with Adam optimization and reduce it by 5% after each epoch. For MinkowskiNet, we use coordinates and intensity as input features and the learning rate is set at 0.001 for SGD optimizer with a weight decay at 1e-4.

5.4. Experimental Results

SemanticKITTI: We first evaluate how SynLiDAR augments SemanticKITTI with RandLA-Net [19] and MinkowskiNet [10] as shown in Tables 2 and 3. We can observe that incorporating SynLiDAR helps train better models for both two networks. This is more obvious for foreground classes with fewer points, which shows that SynLiDAR shares certain similarities with real-world dataset Se-

SemanticKITTI [5]	100%	0%	20%	40%	60%	100%
SynLiDAR	-	✓	✓	✓	✓	✓
mIoU	52.6	20.3	41.2	45.9	53.0	53.6

Table 4: SynLiDAR can replace real data: By including SynLiDAR, up to 40% real data from SemanticKITTI [5] can be removed without sacrificing the performance of the trained semantic segmentation models.

model	train	test	translation	person	rider	car	trunk	plants	traffic sign	pole	garbage-can	building	cone/stone	fence	bike	ground	mIoU
RandLA-Net	P	P	-	44.7	23.4	41.9	34.8	67.8	21.0	21.7	2.2	55.9	16.3	40.8	41.0	85.8	38.3
	P+S	P	-	46.1	27.1	44.4	36.9	69.1	18.0	25.8	3.2	63.7	14.3	41.7	42.6	84.5	39.8
	P+S	P	NDF [47]	48.6	27.6	43.6	35.4	70.7	19.9	22.9	4.4	63.1	19.2	38.6	44.5	83.9	40.2
	P+S	P	PCT-Net (our's)	53.3	38.2	34.7	44.1	69.8	26.2	29.0	11.0	69.6	28.4	38.0	43.3	84.1	43.8

Table 5: Incorporating SynLiDAR with real point cloud data trains better segmentation models: For RandLA-Net [19], including SynLiDAR into the SemanticPOSS [33] training data helps to train more accurate semantic segmentation models. ‘P’ and ‘S’ represent SemanticPOSS and SynLiDAR datasets. ‘NDF’ refers to noise distribution fixing method.

semanticKITTI. For RandLA-Net, including SynLiDAR improves mIoU by 1.0% where foreground classes *motorcycle*, *truck*, and *other-vehicle* improve significantly by 8.1%, 4.9% and 5.9%, respectively. For MinkowskiNet, including SynLiDAR improves mIoU by 1.5% where classes *truck* and *person* improve 5.9% and 5%, respectively.

Fig. 5 shows qualitative results with RandLA-Net. It can be seen that incorporating SynLiDAR in training helps train more powerful models. Specifically, SynLiDAR provides more training samples for some classes such as *person* that has very limited training data in SemanticKITTI. SynLiDAR thus augments SemanticKITTI with better identification of *textit{person}* as shown in zoomed areas in Column 1. Similarly, *other-vehicle* are also better detected with more synthetic samples as illustrated in Column 2.

We further evaluate the proposed PCT-Net and benchmark it with NDF [47] which counts frequency of blank pixels in the projected depth images of KITTI [14] and accordingly drops out pixels in synthetic data. As the two tables show, NDF is not quite effective with only 0.3% mIoU improvement while including its modified SynLiDAR data in training. This is largely because NDF adopts a statistic way to simulate sparsity of LiDAR point cloud while sparsity is highly related to semantic information which cannot be fully represented as statistical frequencies. As a comparison, PCT-Net sees 1.5% and 1.6% mIoU improvements while including its translated SynLiDAR in training, demonstrating the effectiveness of PCT-Net in mitigating domain gap between SynLiDAR and SemanticKITTI.

Besides data augmentation, SynLiDAR can replace a

certain amount of real data and accordingly mitigates the data collection and annotation challenge. We evaluate it by replacing certain amount of SemanticKITTI data with SynLiDAR and train models using RandLA-Net. Specifically, we randomly sampling SemanticKITTI to build an arithmetic real data volume. The selected subset is then combined with SynLiDAR for model training. Table 4 shows experimental results. We can observe that including SynLiDAR can save 40% SemanticKITTI training data with similar no performance sacrifice, demonstrating its effectiveness in reducing manually annotated training data. **SemanticPOSS:** We also performed evaluation over SemanticPOSS that is collected under a different LiDAR sensor setup [1]. As Tables 5 and 6 show, incorporating our SynLiDAR can similarly boost semantic segmentation performance. Specifically, RandLA-Net improves mIoU by 1.5% after including SynLiDAR in training. The mIoU of most classes (10 of 13) increases and it is greatly improved by 7.8% for *building* class. MinkowskiNet improves mIoU by 2.3% after including SynLiDAR in training. All classes improve and the *rider* class is improved by 6.5%.

In addition, PCT-Net mitigates domain gaps between SynLiDAR and SemanticPOSS effectively and it improves mIoU by 4% and 2% for RandLA-Net and MinkowskiNet, respectively. NDF instead improves by 0.4% and 0.6% only.

6. Conclusion

This paper presents SynLiDAR and a point cloud translation network PCT-Net for synthetic-to-real point cloud

model	train	test	translation	person	rider	car	trunk	plants	traffic sign	pole	garbage-can	building	cone/stone	fence	bike	ground	mIoU
MinkNet	P	P	-	55.8	34.1	54.9	30.1	73.5	36.0	26.6	0.2	70.5	0.0	49.5	49.0	78.5	43.0
	P+S	P	-	58.3	40.6	59.4	34.8	74.1	37.7	30.5	0.8	72.0	0.2	51.5	50.3	78.9	45.3
	P+S	P	NDF [47]	59.7	47.9	55.3	31.2	73.9	37.0	33.6	3.0	71.8	0.0	55.1	49.7	78.3	45.9
	P+S	P	PCT-Net (our's)	61.6	50.2	59.1	35.4	74.0	38.8	35.9	4.3	71.7	0.1	56.0	49.9	78.2	47.3

Table 6: Incorporating SynLiDAR with real point cloud data trains better segmentation models: For MinkNet [10], including SynLiDAR into the SemanticPOSS [33] training data helps to train more accurate semantic segmentation models. ‘P’ and ‘S’ represent SemanticPOSS and SynLiDAR datasets. ‘NDF’ refers to noise distribution fixing method.

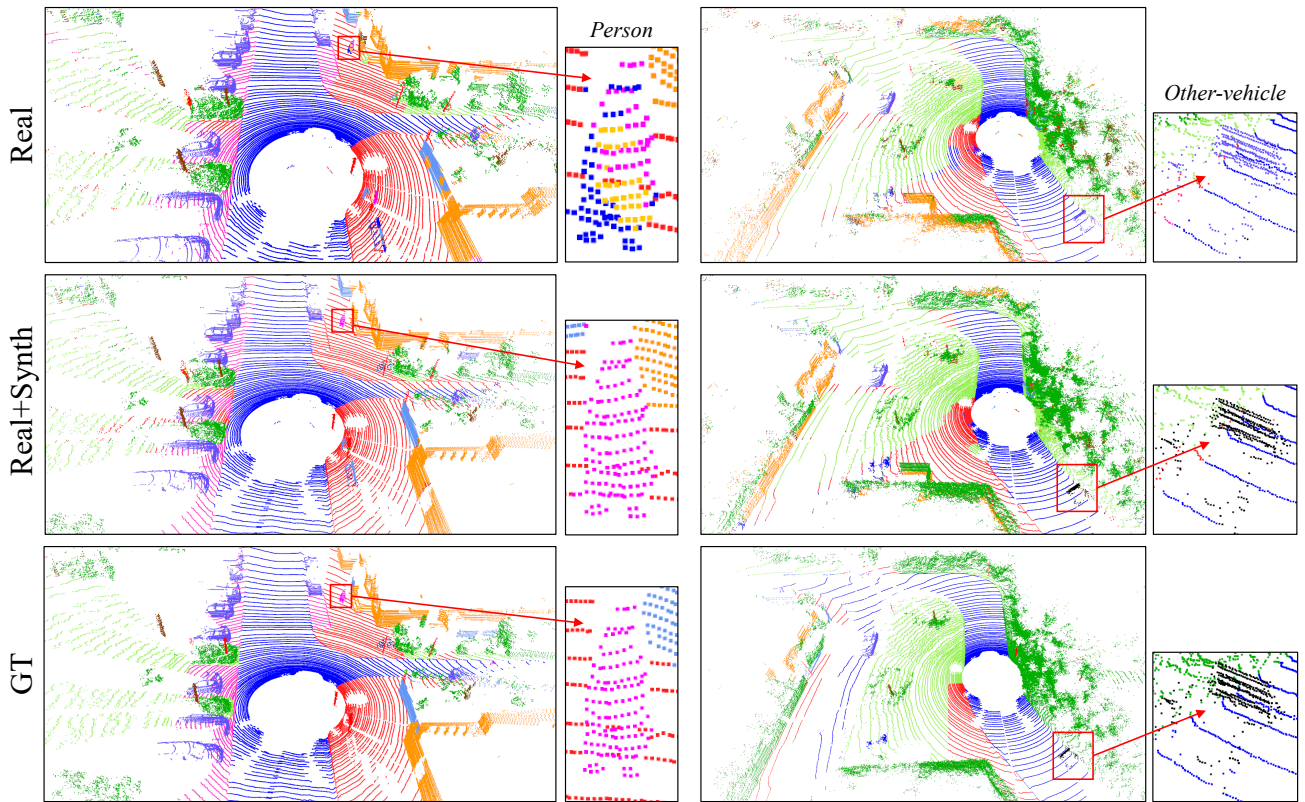


Figure 5: Incorporating SynLiDAR helps train better segmentation models: The three rows show semantic segmentation by SemanticKITTI trained model, SemanticKITTI+SynLiDAR trained model, and ground truth, respectively. Including SynLiDAR helps train better models clearly as illustrated by *person* and *Other-vehicle* in the two samples.

translation. SynLiDAR is a large-scale synthetic LiDAR sequential point cloud dataset that has 19 billion points and point-wise annotations of 32 semantic classes. PCT-Net translates synthetic point clouds to have similar appearance and sparsity as real point clouds. Extensive experiments showed that SynLiDAR shares high geometrical similarities with real-world data, which effectively boosts semantic

segmentation while combining with real data or greatly reduces the amount of annotated real data without sacrificing accuracy. PCT-Net mitigates synthetic-to-real gaps effectively and its translated data further improves point-cloud segmentation consistently. In the future, we will continue to study synthetic-to-real transfer learning methods for LiDAR point cloud.

References

- [1] Hesai pandar40 lidar sensor. <https://www.hesaitech.com/en/Pandar40> Accessed March 15, 2021. **7**
- [2] Unreal game engine. <https://www.unrealengine.com/en-US/what-is-unreal-engine-4> Accessed March 15, 2021. **3**
- [3] Panos Achlioptas, Olga Diamanti, Ioannis Mitliagkas, and Leonidas Guibas. Learning representations and generative models for 3d point clouds. In *International conference on machine learning*, pages 40–49. PMLR, 2018. **4**
- [4] Iro Armeni, Ozan Sener, Amir R Zamir, Helen Jiang, Ioannis Brilakis, Martin Fischer, and Silvio Savarese. 3d semantic parsing of large-scale indoor spaces. In *Proceedings of the IEEE Conference on Computer Vision and Pattern Recognition*, pages 1534–1543, 2016. **2**
- [5] Jens Behley, Martin Garbade, Andres Milioto, Jan Quenzel, Sven Behnke, Cyrill Stachniss, and Jurgen Gall. Semantickitti: A dataset for semantic scene understanding of lidar sequences. In *Proceedings of the IEEE International Conference on Computer Vision*, pages 9297–9307, 2019. **1, 2, 3, 4, 6, 7**
- [6] Holger Caesar, Varun Bankiti, Alex H Lang, Sourabh Vora, Venice Erin Liong, Qiang Xu, Anush Krishnan, Yu Pan, Giancarlo Baldan, and Oscar Beijbom. nuscenes: A multimodal dataset for autonomous driving. In *Proceedings of the IEEE/CVF Conference on Computer Vision and Pattern Recognition*, pages 11621–11631, 2020. **2, 3**
- [7] Xuelin Chen, Baoquan Chen, and Niloy J Mitra. Unpaired point cloud completion on real scans using adversarial training. *arXiv preprint arXiv:1904.00069*, 2019. **4**
- [8] Yunje Choi, Minje Choi, Munyoung Kim, Jung-Woo Ha, Sunghun Kim, and Jaegul Choo. Stargan: Unified generative adversarial networks for multi-domain image-to-image translation. In *Proceedings of the IEEE conference on computer vision and pattern recognition*, pages 8789–8797, 2018. **3**
- [9] Christopher Choy, JunYoung Gwak, and Silvio Savarese. 4d spatio-temporal convnets: Minkowski convolutional neural networks. In *Proceedings of the IEEE/CVF Conference on Computer Vision and Pattern Recognition*, pages 3075–3084, 2019. **2**
- [10] Christopher Choy, JunYoung Gwak, and Silvio Savarese. 4d spatio-temporal convnets: Minkowski convolutional neural networks. In *Proceedings of the IEEE/CVF Conference on Computer Vision and Pattern Recognition*, pages 3075–3084, 2019. **4, 6, 8**
- [11] Peng Dai, Yinda Zhang, Zhuwen Li, Shuaicheng Liu, and Bing Zeng. Neural point cloud rendering via multi-plane projection. In *Proceedings of the IEEE/CVF Conference on Computer Vision and Pattern Recognition*, pages 7830–7839, 2020. **3**
- [12] Haoqiang Fan, Hao Su, and Leonidas J Guibas. A point set generation network for 3d object reconstruction from a single image. In *Proceedings of the IEEE conference on computer vision and pattern recognition*, pages 605–613, 2017. **4, 5**
- [13] Adrien Gaidon, Qiao Wang, Yann Cabon, and Eleonora Vig. Virtual worlds as proxy for multi-object tracking analysis. In *Proceedings of the IEEE conference on computer vision and pattern recognition*, pages 4340–4349, 2016. **2**
- [14] Andreas Geiger, Philip Lenz, Christoph Stiller, and Raquel Urtasun. Vision meets robotics: The kitti dataset. *The International Journal of Robotics Research*, 32(11):1231–1237, 2013. **7**
- [15] Andreas Geiger, Philip Lenz, and Raquel Urtasun. Are we ready for autonomous driving? the kitti vision benchmark suite. In *2012 IEEE Conference on Computer Vision and Pattern Recognition*, pages 3354–3361. IEEE, 2012. **3**
- [16] Benjamin Graham, Martin Engelcke, and Laurens Van Der Maaten. 3d semantic segmentation with submanifold sparse convolutional networks. In *Proceedings of the IEEE conference on computer vision and pattern recognition*, pages 9224–9232, 2018. **2**
- [17] Yulan Guo, Hanyun Wang, Qingyong Hu, Hao Liu, Li Liu, and Mohammed Bennamoun. Deep learning for 3d point clouds: A survey. *IEEE transactions on pattern analysis and machine intelligence*, 2020. **2**
- [18] Lei Han, Tian Zheng, Lan Xu, and Lu Fang. Occuseg: Occupancy-aware 3d instance segmentation. In *Proceedings of the IEEE/CVF conference on computer vision and pattern recognition*, pages 2940–2949, 2020. **2**
- [19] Qingyong Hu, Bo Yang, Linhai Xie, Stefano Rosa, Yulan Guo, Zhihua Wang, Niki Trigoni, and Andrew Markham. Randla-net: Efficient semantic segmentation of large-scale point clouds. In *Proceedings of the IEEE/CVF Conference on Computer Vision and Pattern Recognition*, pages 11108–11117, 2020. **1, 2, 6, 7**
- [20] Xun Huang, Ming-Yu Liu, Serge Belongie, and Jan Kautz. Multimodal unsupervised image-to-image translation. In *Proceedings of the European conference on computer vision (ECCV)*, pages 172–189, 2018. **3**
- [21] Zitian Huang, Yikuan Yu, Jiawen Xu, Feng Ni, and Xinyi Le. PF-net: Point fractal network for 3d point cloud completion. In *Proceedings of the IEEE/CVF Conference on Computer Vision and Pattern Recognition*, pages 7662–7670, 2020. **4**
- [22] Braden Hurl, Krzysztof Czarnecki, and Steven Waslander. Precise synthetic image and lidar (presil) dataset for autonomous vehicle perception. In *2019 IEEE Intelligent Vehicles Symposium (IV)*, pages 2522–2529. IEEE, 2019. **2, 3**
- [23] Phillip Isola, Jun-Yan Zhu, Tinghui Zhou, and Alexei A Efros. Image-to-image translation with conditional adversarial networks. In *Proceedings of the IEEE conference on computer vision and pattern recognition*, pages 1125–1134, 2017. **3**
- [24] Deyvid Kochanov, Fatemeh Karimi Nejadasl, and Olaf Booi. Kprnet: Improving projection-based lidar semantic segmentation. *arXiv preprint arXiv:2007.12668*, 2020. **2**
- [25] Elyor Kodirov, Tao Xiang, Zhenyong Fu, and Shaogang Gong. Unsupervised domain adaptation for zero-shot learning. In *Proceedings of the IEEE international conference on computer vision*, pages 2452–2460, 2015. **2**

- [26] Ruihui Li, Xianzhi Li, Chi-Wing Fu, Daniel Cohen-Or, and Pheng-Ann Heng. Pu-gan: a point cloud upsampling adversarial network. In *Proceedings of the IEEE/CVF International Conference on Computer Vision*, pages 7203–7212, 2019. 4, 6
- [27] Fayao Liu, Chunhua Shen, and Guosheng Lin. Deep convolutional neural fields for depth estimation from a single image. In *Proceedings of the IEEE conference on computer vision and pattern recognition*, pages 5162–5170, 2015. 3
- [28] Ming-Yu Liu, Xun Huang, Arun Mallya, Tero Karras, Timo Aila, Jaakko Lehtinen, and Jan Kautz. Few-shot unsupervised image-to-image translation. In *Proceedings of the IEEE/CVF International Conference on Computer Vision*, pages 10551–10560, 2019. 3
- [29] Zhijian Liu, Haotian Tang, Yujun Lin, and Song Han. Point-voxel cnn for efficient 3d deep learning. *arXiv preprint arXiv:1907.03739*, 2019. 2
- [30] Sivabalan Manivasagam, Shenlong Wang, Kelvin Wong, Wenyuan Zeng, Mikita Sazanovich, Shuhan Tan, Bin Yang, Wei-Chiu Ma, and Raquel Urtasun. Lidarsim: Realistic lidar simulation by leveraging the real world. In *Proceedings of the IEEE/CVF Conference on Computer Vision and Pattern Recognition*, pages 11167–11176, 2020. 3
- [31] Youssef A Mejjati, Christian Richardt, James Tompkin, Darren Cosker, and Kwang In Kim. Unsupervised attention-guided image to image translation. *arXiv preprint arXiv:1806.02311*, 2018. 3
- [32] Andres Milioto, Ignacio Vizzo, Jens Behley, and Cyrill Stachniss. Rangenet++: Fast and accurate lidar semantic segmentation. In *2019 IEEE/RSJ International Conference on Intelligent Robots and Systems (IROS)*, pages 4213–4220. IEEE, 2019. 1, 2
- [33] Yancheng Pan, Biao Gao, Jilin Mei, Sibogeng, Chengkun Li, and Huijing Zhao. Semanticpos: A point cloud dataset with large quantity of dynamic instances. *arXiv preprint arXiv:2002.09147*, 2020. 1, 2, 3, 4, 6, 7, 8
- [34] Albert Pumarola, Stefan Popov, Francesc Moreno-Noguer, and Vittorio Ferrari. C-flow: Conditional generative flow models for images and 3d point clouds. In *Proceedings of the IEEE/CVF Conference on Computer Vision and Pattern Recognition*, pages 7949–7958, 2020. 3
- [35] Charles R Qi, Hao Su, Kaichun Mo, and Leonidas J Guibas. Pointnet: Deep learning on point sets for 3d classification and segmentation. In *Proceedings of the IEEE conference on computer vision and pattern recognition*, pages 652–660, 2017. 2
- [36] Charles R Qi, Li Yi, Hao Su, and Leonidas J Guibas. Pointnet++: Deep hierarchical feature learning on point sets in a metric space. *arXiv preprint arXiv:1706.02413*, 2017. 2
- [37] Stephan R Richter, Vibhav Vineet, Stefan Roth, and Vladlen Koltun. Playing for data: Ground truth from computer games. In *European conference on computer vision*, pages 102–118. Springer, 2016. 3
- [38] German Ros, Laura Sellart, Joanna Materzynska, David Vazquez, and Antonio M Lopez. The synthia dataset: A large collection of synthetic images for semantic segmentation of urban scenes. In *Proceedings of the IEEE conference on computer vision and pattern recognition*, pages 3234–3243, 2016. 2
- [39] Riccardo Roveri, Lukas Rahmann, Cengiz Oztireli, and Markus Gross. A network architecture for point cloud classification via automatic depth images generation. In *Proceedings of the IEEE Conference on Computer Vision and Pattern Recognition*, pages 4176–4184, 2018. 3
- [40] Kuniaki Saito, Donghyun Kim, Stan Sclaroff, Trevor Darrell, and Kate Saenko. Semi-supervised domain adaptation via minimax entropy. In *Proceedings of the IEEE/CVF International Conference on Computer Vision*, pages 8050–8058, 2019. 2
- [41] Kuniaki Saito, Kohei Watanabe, Yoshitaka Ushiku, and Tatsuya Harada. Maximum classifier discrepancy for unsupervised domain adaptation. In *Proceedings of the IEEE conference on computer vision and pattern recognition*, pages 3723–3732, 2018. 2
- [42] Shital Shah, Debadeepta Dey, Chris Lovett, and Ashish Kapoor. Airsim: High-fidelity visual and physical simulation for autonomous vehicles. In *Field and Service Robotics*, 2017. 3
- [43] Ruoqi Sun, Xinge Zhu, Chongruo Wu, Chen Huang, Jianping Shi, and Lizhuang Ma. Not all areas are equal: Transfer learning for semantic segmentation via hierarchical region selection. In *Proceedings of the IEEE Conference on Computer Vision and Pattern Recognition*, pages 4360–4369, 2019. 2
- [44] Haotian Tang, Zhijian Liu, Shengyu Zhao, Yujun Lin, Ji Lin, Hanrui Wang, and Song Han. Searching efficient 3d architectures with sparse point-voxel convolution. In *European Conference on Computer Vision*, pages 685–702. Springer, 2020. 1, 2
- [45] Hugues Thomas, Charles R Qi, Jean-Emmanuel Deschaud, Beatriz Marcotequi, François Goulette, and Leonidas J Guibas. Kpconv: Flexible and deformable convolution for point clouds. In *Proceedings of the IEEE/CVF International Conference on Computer Vision*, pages 6411–6420, 2019. 2
- [46] Ting-Chun Wang, Ming-Yu Liu, Jun-Yan Zhu, Andrew Tao, Jan Kautz, and Bryan Catanzaro. High-resolution image synthesis and semantic manipulation with conditional gans. In *Proceedings of the IEEE conference on computer vision and pattern recognition*, pages 8798–8807, 2018. 3
- [47] Bichen Wu, Alvin Wan, Xiangyu Yue, and Kurt Keutzer. Squeezeseg: Convolutional neural nets with recurrent crf for real-time road-object segmentation from 3d lidar point cloud. In *2018 IEEE International Conference on Robotics and Automation (ICRA)*, pages 1887–1893. IEEE, 2018. 2, 3, 6, 7, 8
- [48] Bichen Wu, Xuanyu Zhou, Sicheng Zhao, Xiangyu Yue, and Kurt Keutzer. Squeezesegv2: Improved model structure and unsupervised domain adaptation for road-object segmentation from a lidar point cloud. In *2019 International Conference on Robotics and Automation (ICRA)*, pages 4376–4382. IEEE, 2019. 2
- [49] Jiajun Wu, Chengkai Zhang, Tianfan Xue, William T Freeman, and Joshua B Tenenbaum. Learning a probabilistic latent space of object shapes via 3d generative-adversarial modeling. *arXiv preprint arXiv:1610.07584*, 2016. 4

- [50] David Yoon, Tim Tang, and Timothy Barfoot. Mapless on-line detection of dynamic objects in 3d lidar. In *2019 16th Conference on Computer and Robot Vision (CRV)*, pages 113–120. IEEE, 2019. 3
- [51] Feihu Zhang, Jin Fang, Benjamin Wah, and Philip Torr. Deep fusionnet for point cloud semantic segmentation. In *ECCV*, volume 2, page 6, 2020. 2
- [52] Yang Zhang, Zixiang Zhou, Philip David, Xiangyu Yue, Zerong Xi, Boqing Gong, and Hassan Foroosh. Polarnet: An improved grid representation for online lidar point clouds semantic segmentation. In *Proceedings of the IEEE/CVF Conference on Computer Vision and Pattern Recognition*, pages 9601–9610, 2020. 2
- [53] Chuanxia Zheng, Tat-Jen Cham, and Jianfei Cai. T2net: Synthetic-to-realistic translation for solving single-image depth estimation tasks. In *Proceedings of the European Conference on Computer Vision (ECCV)*, pages 767–783, 2018. 3
- [54] Jun-Yan Zhu, Taesung Park, Phillip Isola, and Alexei A Efros. Unpaired image-to-image translation using cycle-consistent adversarial networks. In *Proceedings of the IEEE international conference on computer vision*, pages 2223–2232, 2017. 3, 6
- [55] Jun-Yan Zhu, Richard Zhang, Deepak Pathak, Trevor Darrell, Alexei A Efros, Oliver Wang, and Eli Shechtman. Toward multimodal image-to-image translation. *arXiv preprint arXiv:1711.11586*, 2017. 3
- [56] Xinge Zhu, Hui Zhou, Tai Wang, Fangzhou Hong, Yuexin Ma, Wei Li, Hongsheng Li, and Dahua Lin. Cylindrical and asymmetrical 3d convolution networks for lidar segmentation. *arXiv preprint arXiv:2011.10033*, 2020. 2, 4